

In-vivo operation of the Boston 15-channel wireless subretinal visual prosthesis

Douglas B. Shire*^{a,b}, Patrick Doyle^{b,c}, Shawn K. Kelly^{b,c}, Marcus D. Gingerich^{a,b}, Jinghua Chen^d,
Stuart F. Cogan^e, William A. Drohan^{b,c}, Oscar Mendoza^c, Luke Theogarajan^f,
John Wyatt^c, and Joseph F. Rizzo^{b,d}

^aCornell University/CNF, 119 Phillips Hall, Ithaca, NY USA 14853-5401;

^bCenter for Innovative Visual Rehabilitation (CIVR), Boston VA Healthcare System,
150 S. Huntington Avenue, Mailstop 151E, Boston, MA USA 02130;

^cMassachusetts Institute of Technology, Research Laboratory of Electronics,
Building 36-576, 50 Vassar Street, Cambridge, MA USA 02139;

^dMassachusetts Eye and Ear Infirmary, 243 Charles Street, Boston, MA USA 02114;

^eEIC Laboratories, Inc., 111 Downey Street, Norwood, MA USA 02062;

^fElectrical & Computer Engineering Dept., University of California, Santa Barbara, CA USA 93106

ABSTRACT

This presentation concerns the engineering development of the Boston visual prosthesis for restoring useful vision to patients blind with degenerative retinal disease. A miniaturized, hermetically-encased, 15-channel wirelessly-operated retinal prosthetic was developed for implantation and pre-clinical studies in Yucatan mini-pig animal models. The prosthesis conforms to the eye and drives a microfabricated polyimide stimulating electrode array having sputtered iridium oxide electrodes. This array is implanted into the subretinal space using a specially-designed *ab externo* surgical technique; the bulk of the prosthesis is on the surface of the sclera. The implanted device includes a hermetic titanium case containing a 15-channel stimulator chip; secondary power/data receiving coils surround the cornea. Long-term *in vitro* pulse testing was also performed on the electrodes to ensure their stability over years of operation. Assemblies were first tested *in vitro* to verify wireless operation of the system in biological saline using a custom RF transmitter circuit and primary coils. Stimulation pulse strength, duration and frequency were programmed wirelessly using a computer with a custom graphical user interface. Operation of the retinal implant was verified *in vivo* in 3 minipigs for more than three months by measuring stimulus artifacts on the eye surface using contact lens electrodes.

Keywords: Retinal prosthesis, Visual prosthetic, retinal implant, wireless, implantable, subretinal, hermetic

1. INTRODUCTION

Retinal prostheses are actively being developed by a number of groups worldwide¹⁻¹². These devices aim to restore visual function lost due to degenerative retinal diseases such as retinitis pigmentosa (RP) and age-related macular degeneration (AMD). These conditions cause a gradual loss of photoreceptors, yet a substantial fraction of the retinal ganglion cells remain, forming intact neural pathways from the retina to the visual cortex. The prevalence of RP is approximately 1 in every 4000 live births, and there are approximately 1,700,000 affected individuals worldwide. AMD is the leading cause of blindness in the developed world, with roughly 2 million affected patients in the United States alone. This number is expected to increase by 50% by the year 2020 as the population ages¹³. Existing treatments at best slow the progress of these diseases, but no cure is known. While it is evident that significant reorganization of the retina occurs after the loss of input signals from the photoreceptors¹⁴, our group and others have nevertheless demonstrated that focal electrical stimulation of the retinal ganglion cells can yield responses which correspond to the

*dbs6@cornell.edu; Tel. +1 (607) 255-2449; FAX +1 (607) 255-8601; <http://www.bostonretinalimplant.org>

strength and location of the stimuli¹⁵. However, threshold currents sufficient to elicit phosphenes have been found to be higher than normal in subjects with retinal degeneration². It became evident to our team after acute human surgical studies that a chronically implantable device was required to fully explore the prospects of returning useful vision. Indeed, other groups are also actively engaged in similar efforts⁸⁻¹².

The majority of the groups working in visual prosthetics today are concentrating either on direct epiretinal^{4,5} or subretinal^{6,7} electrical stimulation, or less direct stimulation of the retina using a supra-choroidal or trans-scleral approach⁸⁻¹⁰. Our team's approach for a number of years focused on epiretinal prosthesis design, culminating in several acute human surgical trials using flexible, polyimide-based stimulating electrode arrays comparable to those in our present design^{2,3}. A number of factors, however, led to our group decision to take an *ab externo*, subretinal surgical approach to chronic implantation of a wirelessly driven microstimulator. This design approach yields improved biocompatibility, a less-invasive surgery, and leaves the bulk of the implant device outside the eye.

Our first-generation wirelessly-powered implantable retinal stimulation device was implanted in Yucatan mini-pigs during the spring and summer of 2008¹. We describe here an improved version of the implant, with the circuits encased in a hermetic titanium enclosure, the coils moved to a more magnetically-favorable position, and easier surgical access for electrode array insertion. We have also performed significantly more testing of our thin-film microfabricated electrode array.

2. RETINAL IMPLANT DESIGN AND METHODS

2.1 System Description

Our implant system consists of a computer-based controller with a user interface for selecting which electrodes to drive with which level of current. Data from the computer system is sent to a power amplifier, from which it is transmitted wirelessly to the implant by near-field inductive coupling. Data at 100 Kbps are encoded by amplitude shift keying on a 15.5 MHz carrier. Power is also wirelessly transmitted to the implant, using a 125 KHz carrier, rectified by the implant to create ± 2.5 V power supplies. A system overview is shown in Figure 1, below.

The implant itself is attached to the outside of the eye, where it receives and processes the power and data, and sends electrical stimulation current to the retinal nerve cells via a thin-film microfabricated array of sputtered iridium oxide film (SIROF) electrodes, surgically inserted into the subretinal space through a flap in the sclera.

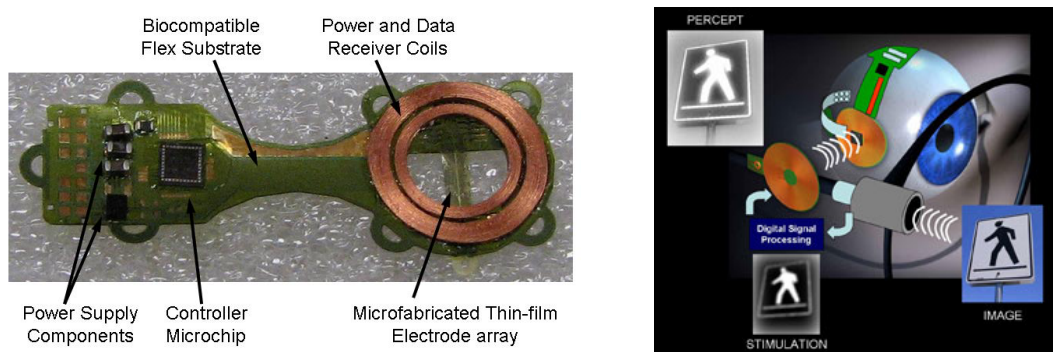


Figure 1. Left: first-generation retinal prosthesis. This flexible device wraps around the eye, and the electrode array inserts through a flap in the sclera to access the subretinal space. The power and data transmitting coils rest on glasses. Right: An overview of the operation of the retinal prosthesis system. Images of the patient's environment are captured by a small video camera mounted on a pair of eyeglasses. A portable patient control unit containing digital signal processing hardware converts the image to a series of current pulse commands that are then wirelessly transmitted to the implant. Pixels corresponding to lighter and darker areas of the patient's surroundings are then stimulated by the implant using a microfabricated electrode array that is inserted into the subretinal space.

2.2 Differences from First-Generation Device

Our first-generation device was assembled on a flexible substrate that wrapped around the eye, attaching to the sclera of the eye, inside the socket¹ (see Figure 1). This device had three significant design drawbacks: (1) small receiver coils made power and data telemetry difficult, (2) the silicone coating held up well in studies of a few months, but would not be viable for chronic trials of many years, and (3) the required surgical approach for electrode array insertion is very difficult. In addition, we had relatively little data about the long-term survivability of our electrode arrays under continuous stimulation.

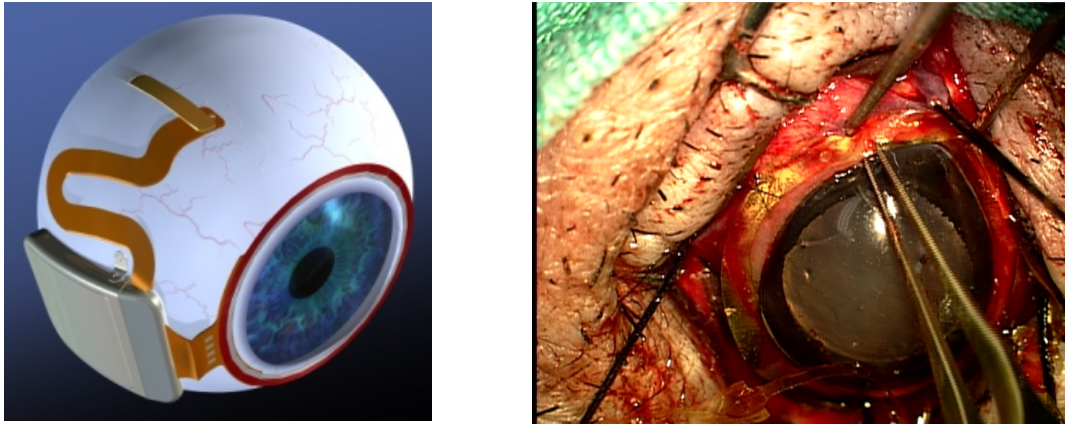


Figure 2. Left: drawing of hermetic implant concept. The power and data receiver coils are now on the front of the eye, just behind the conjunctiva. The electronics are enclosed in a hermetic titanium case, and the electrode array insertion is in its own quadrant for ease of surgical access. Right: photo taken during surgical implantation of the device in a Yucatan mini-pig eye.

Our newer-generation device uses the same controller chip¹⁶ and power and data telemetry scheme, but solves the three problems outlined above, with: (1) larger coils, conforming to the eye, surrounding the cornea, just behind the conjunctiva, (2) a hermetic, titanium case enclosing the circuitry, attached to the sclera deep in the superior-nasal quadrant, and (3) a serpentine electrode array which extends from the case to the superior-temporal quadrant, giving open surgical access to create the scleral flap and insert the array into the subretinal space. The concept of this hermetic implant is shown in Figure 2, together with a photo taken during animal implantation surgery.

2.3 Improved Implant Components

Relocating the secondary power and data coils from the temporal side of the eye to the anterior of the eye allowed for much larger coils, giving much better inductive coupling. However, these coils are against the delicate conjunctiva, and can wear through, creating the risk of infection. Thus the coils are carefully wound on a sphere so that they match the curvature of the eye. The secondary coils include both power and data, but are wound together for structural support. They are made of 40 AWG gold wire, with 28 turns for the power coil and two 6-turn coils for a 12-turn center-tapped data receiver. The spherical-molded coil has a mean radius of 9.5 mm, and a thickness off of the eye of less than 0.2 mm. The secondary coils are shown on a model eye in Figure 3.

The integrated circuit, which includes the telemetry receiver, digital controller, analog current sources, biases, and startup circuitry, is encased in the curved titanium enclosure measuring 11 mm x 11 mm x 2 mm. Additionally, schottky rectifier diodes, two power supply capacitors, a discrete resistor and capacitor for power-up reset delay, a resonating capacitor for the power secondary coil, and a 5.1 V zener diode for power supply regulation are included in the package. The circuit board included in the hermetic package is shown in Figure 4.

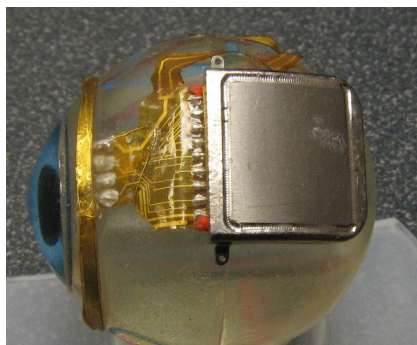


Figure 3. Hermetic retinal prosthesis, a prototype of the device in Figure 2. The gold power and data secondary coils are wound on a sphere to match the eye curvature. The machined titanium case with welded lid has a hermetic ceramic feedthrough. The electrode array is out of view over the top of the eye.

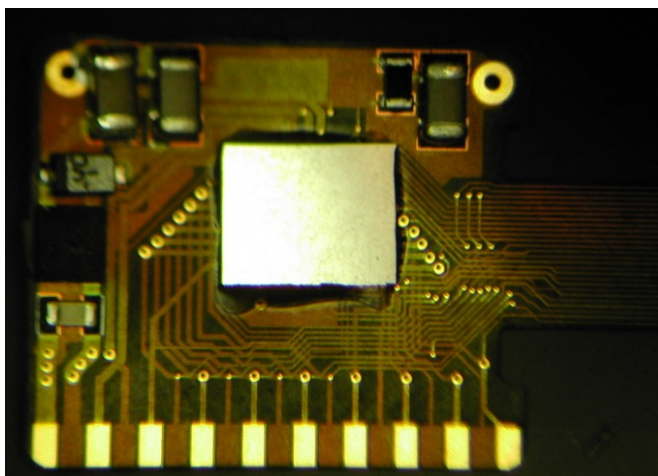


Figure 4. Retinal implant circuit board. The controller IC, as well as power supply and signal conditioning components, are inserted into the curved hermetic titanium case.

The novel, serpentine design of our flexible, thin-film electrode array allows the surgeon to route it behind the superior rectus muscle and insert the electrodes into the superior-temporal quadrant. Since the titanium case is in the superior-nasal quadrant and the secondary coil has a low profile, nothing blocks surgical access to the scleral flap.

2.4 Long-term Electrode Pulsing

Encasing the electronics in a hermetically-sealed titanium envelope allows us to implant this device for a much longer time than the first-generation device. This longer-term implantation requires additional testing of the microfabricated, reactively-sputtered iridium oxide (SIROF) electrodes under chronic pulsing conditions. To assess their stability for chronic animal implantation, we subjected SIROF electrodes to long-term *in vitro* pulsing. Arrays with sixteen 400 μm diameter electrodes were pulsed at 37°C in an inorganic model of interstitial fluid¹⁷. The multichannel stimulators for *in vitro* pulsing employed circuits generating electrical current pulse protocols similar to those used in the implant for animal testing. Eight electrodes on each array were pulsed at a charge density of 200 $\mu\text{C}/\text{cm}^2$ (1 ms pulse width, 50 Hz repetition rate) using a +0.6 V (vs. Ag/AgCl) interpulse bias¹⁸.

2.5 Implant Testing

The full implant system was tested dry on the bench, and *in vitro* in a phosphate buffered saline solution. Electrodes were driven with balanced biphasic pulses of current, 25-200 μA per phase, with each phase lasting 1 msec. Similar stimulation parameters were used during *in vivo* stimulation trials performed in the Yucatan mini-pig.

During wireless *in vitro* tests, no test points were available to access the circuitry, so two needle electrodes were immersed into the saline, and a differential voltage was measured with a custom-built instrumentation amplifier to measure stimulus artifacts. The same type of measurement was made *in vivo*, instead using a contact lens electrode and a reference electrode on the animal's ear, to ensure that the device remained working in the pig eye. These measurements were entirely non-invasive.

3. RESULTS

3.1 Long-term Electrode Pulsing

An example of the voltage transients from eight electrodes on one array and a representative current waveform are shown in Figure 5. The voltage transients are quite similar for the eight electrodes with maximum cathodal potential (Emc) of about 0.4 V Ag/AgCl, well positive of the -0.6 V water reduction potential on SIROF. Cyclic voltammetry in model interstitial fluid also showed consistency in electrode response and good stability over long term pulsing. In Figure 6, the voltammograms of the eight pulsed electrodes are compared after 670 hr and 2900 hr of pulsing. The origin of the observed changes in the CV response between 670 hr and 2900 hr is uncertain, although the observed changes are consistent with a decrease in the density of the SIROF due to hydration.

3.2 Implant *In Vitro* and *In Vivo* Test Results

A typical electrode test waveform is shown in Figure 7. This type of waveform shows the resistive portions of the fluid and the electrode access resistance, but also the charging of the electrode-tissue interface. Examples from stimulation of the mini-pig eye are shown in Figure 8. These stimulus artifact waveforms show only the voltage arising from current flowing through fluid. The waveforms show a great deal of variance, largely due to inconsistencies in the placement of the contact lens electrode, and the use of a distant reference electrode on the animal's ear. However, this measurement method is non-invasive, and greatly simplified the testing, allowing for non-sterile follow-up studies after surgical implantation of the device.

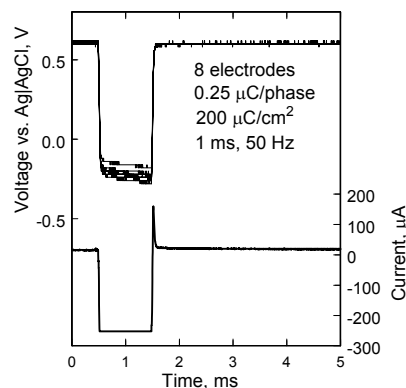


Figure 5. Voltage transients of eight SIROF electrodes on a polyimide array. The electrodes have been pulsed for 2900 hr at $200 \mu\text{C}/\text{cm}^2$. A representative current waveform is also shown.

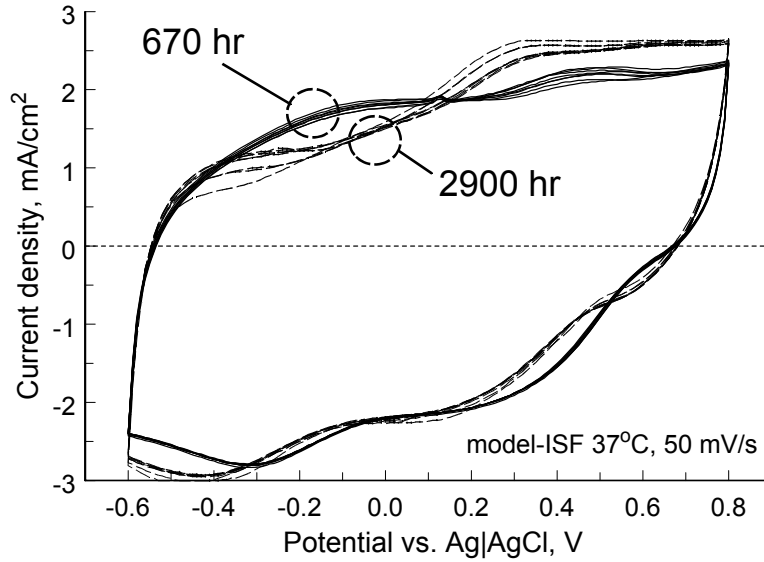


Figure 6. Cyclic voltammograms of eight SIROF electrodes after 670 hr (solid) and 2900 hr (dashed) of pulsing at $200 \mu\text{C}/\text{cm}^2$.

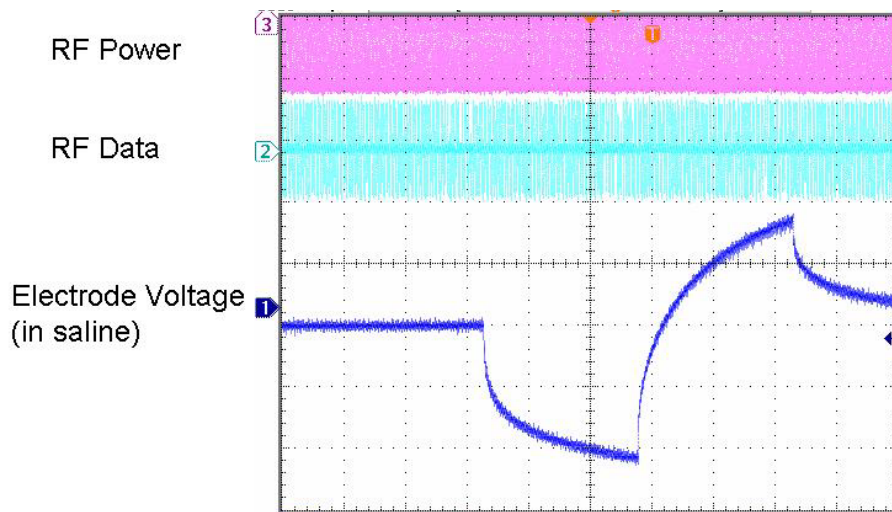


Figure 7. *In vitro* electrode test waveform for a wirelessly-driven implant. The bottom waveform shows the electrode voltage measured in saline via a test tail that is trimmed off prior to surgery.

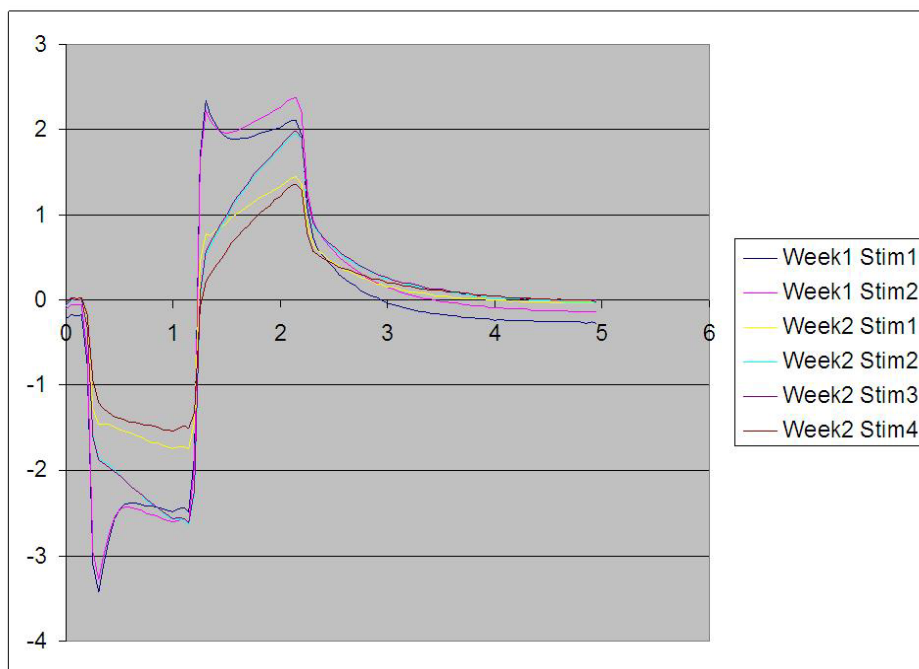


Figure 8. Measured electrical stimulus artifacts from the Yucatan mini-pig eye. The wide variation in waveform size and shape has mostly to do with the variation in placement of the contact lens electrode that was used to record the voltage transients on the eye. The millivolt-level voltage scale is arbitrary; time scale is 1 msec / division.

CONCLUSION

The hermetic implant system presented here is capable of being implanted for a much longer time than our previous silicone-coated implant. This allows for the 5+ year chronic survivability expected by the FDA for future clinical trials of our visual prosthesis. Our device worked reliably during animal testing for over three months, though exposure problems at the conjunctiva forced an early end to the experiment. We have redesigned the coil forming process and the connection between the hermetic case and the receiving coils so as to ease the tension on the conjunctiva in future trials. These modifications will allow longer-term animal implantations in the near future, with a view toward human clinical trials of a subretinal visual prosthesis that will be capable of restoring some useful vision to blind patients.

REFERENCES

- [1] Shire, D. B., Kelly, S. K., Chen, J., Doyle, P., Gingerich, M. D., Cogan, S. F., Drohan, W., Mendoza, O., Theogarajan, L., Wyatt, J. L., and Rizzo, J. F., "Development and ab externo Implantation of a Wirelessly-Driven Sub-Retinal Neurostimulator," *IEEE Trans. Biomed. Eng.*, vol. 56(10), pp. 2502-2511 (2009).

- [2] Rizzo, J. F., Wyatt J., Loewenstein, J., Kelly, S., and Shire, D., "Perceptual Efficacy of Electrical Stimulation of Human Retina with a Microelectrode Array During Short-Term Surgical Trials," *Invest. Ophthalmol. Vis. Sci.*, vol. 44, pp. 5362-5369 (2003).
- [3] Rizzo, J. F., Wyatt, J., Loewenstein, J., Kelly, S., and Shire, D., "Methods and Perceptual Thresholds for Short-Term Electrical Stimulation of Human Retina with Microelectrode Arrays," *Invest. Ophthalmol. Vis. Sci.*, vol. 44, pp. 5355-5361 (2003).
- [4] Yanai, D., Weiland, J. D., Mahadevappa, M., Greenberg, R. J., Fine, I., and Humayun, M. S., "Visual Performance Using a Retinal Prosthesis in Three Subjects with Retinitis Pigmentosa," *Am. J. Ophthalmol.*, vol. 143, pp. 820-827 (2007).
- [5] Gerding, H., Benner, F. P., and Taneri, S., "Experimental Implantation of Epiretinal Retina Implants (EPI-RET) With an IOL-Type Receiver Unit," *J. Neural Eng.*, vol. 4, pp. S38-S49 (2007).
- [6] DeMarco, P. J. Jr., Yarbrough, G. L., Yee, C. W., Mclean, G. Y., Sagdullaev, B. T., Ball, S. L., and McCall, M. A., "Stimulation via a Subretinally Placed Prosthetic Elicits Central Activity and Induces a Trophic Effect on Visual Responses," *Invest. Ophthalmol. Vis. Sci.*, vol. 48, pp. 916-926 (2007).
- [7] Schanze, T., Sachs, H. G., Wiesenack, C., Brunner, U., and Sailer, H., "Implantation and Testing of Subretinal Film Electrodes in Domestic Pigs," *Exp. Eye Res.*, vol. 82, pp. 332-340 (2006).
- [8] Zhou, J. A., Woo, S. J., Park, S. I., Kim, E. T., Seo, J. M., Chung, H., and Kim, S. J., "A Suprachoroidal Electrical Retinal Stimulator Design for Long-Term Animal Experiments and In-Vivo Assessment of its Feasibility and Biocompatibility in Rabbits," *J. Biomed. Biotech.*, vol. 2008, Article ID 547428, 10 pp. (2008).
- [9] Wong, Y. T., Dommel, N., Preston, P., Hallum, L. E., Lehmann, T., Lovell, N. H., and Suaning, G. J., "Retinal Neurostimulator for a Multifocal Vision Prosthesis," *IEEE Trans. Neural Syst. Rehab. Eng.*, vol. 15, pp. 425-434 (2007).
- [10] Terasawa, Y., Tashiro, H., Uehara, A., Saitoh, T., Ozawa, M., Tokuda, T., and Ohta, J., "The Development of a Multichannel Electrode Array for Retinal Prostheses," *J. Artif. Organs*, vol. 9, pp. 263-266 (2006).
- [11] Hornig, R., Zehnder, T., Velikay-Parel, M., Laube, T., Feucht, M., and Richard, G., "The IMI Retinal Implant System," [Artificial Sight: Basic Research, Biomedical Engineering, and Clinical Advances] Springer, New York, 111-128 (2007).
- [12] Zrenner, E., "Restoring Neuroretinal Function: New Potentials," *Doc. Ophthalmol.*, vol. 115, pp. 56-59 (2007).
- [13] Friedman, D., O'Colmain, B., Muñoz, B., Tomany, S. C., McCarty, C., de Jong, P. T., Nemesure, B., Mitchell, P., and Kempen, J., "Prevalence of Age-Related Macular Degeneration in the United States," *Arch. Ophthalmol.*, vol. 122, pp. 564-572 (2004).
- [14] Marc, R. E., Jones, B. W., Anderson, J. R., Kinard, K., Marshak, D. W., Wilson, J. H., Wensel, T. G., and Lucas, R. J., "Neural Reprogramming in Retinal Degenerations," *Invest. Ophthalmol. Vis. Sci.*, vol. 48, pp. 3364-3371 (2007).
- [15] Jensen, R. J., and Rizzo, J. F., "Responses of Ganglion Cells to Repetitive Electrical Stimulation of the Retina," *J. Neural Eng.*, vol. 4, pp. S1-S6 (2007).
- [16] Theogarajan, L. S., "A Low-Power Fully Implantable 15-Channel Retinal Stimulator Chip," *IEEE J. Solid-State Circuits*, vol. 43, pp. 2322-2337 (2008).
- [17] Cogan, S. F., Troyk, P. R., Ehrlich, J., Gasbarro, C. M., and Plante, T. D., "The influence of electrolyte composition on the in vitro charge-injection limits of activated iridium oxide (AIROF) Stimulation Electrodes," *J. Neural Eng.*, vol. 4, pp. 79-86 (2007).
- [18] Cogan, S. F., Troyk, P. R., Ehrlich, J., and Plante, T. D., "In vitro comparison of the charge-injection limits of activated iridium oxide (AIROF) and platinum-iridium microelectrodes," *IEEE Trans Biomed Eng.*, vol. 52, pp. 1612-1614 (2005).